

# BEAM DYNAMICS ANALYSIS AND CORRECTION OF MAGNET FIELD IMPERFECTIONS IN THE SNS ACCUMULATOR RING\*

Y. Papaphilippou<sup>†</sup> and D.T. Abell, BNL, Upton NY 11973, USA

## Abstract

Magnet errors and fringe fields can significantly affect the beam dynamics of the Spallation Neutron Source accumulator ring. Using MARYLIE, we model such effects and generate maps, and corresponding tracking data, and then identify the impact on the beam's non-linear dynamics. To reduce these effects, we propose and compare several possible correction schemes for the SNS accumulator ring.

## 1 INTRODUCTION

The Spallation Neutron Source (SNS) ring [1] will accumulate a high-intensity beam of  $2.1 \times 10^{14}$  protons—a single bunch at a maximum energy of 1.3 GeV—with a transverse emittance  $\epsilon_{x,y} = 160\pi \text{ mm} \cdot \text{mr}$  (at 95%) and a momentum spread  $\delta p/p = \pm 0.7\%$ . A principal design constraint is the low tolerance,  $10^{-4}$ , set for uncontrolled beam loss [2]. From a beam dynamics perspective, the major effects limiting the ring's performance are space-charge forces and magnet field imperfections. Even if space-charge is the dominant concern [3], it is the interaction of space-charge and magnet non-linearities that severely reduces the dynamic aperture. To provide the required acceptance, the SNS ring magnets necessarily have large bores. As the quadrupole magnets have aspect ratios (bore over length) of about 0.5, their fringes make a significant contribution. Here we review some studies undertaken to identify and correct these magnet non-linearities. Special effort has been devoted to the quadrupoles, since their fringe-fields and dodecapole edge errors are the dominant magnet field imperfections in the SNS ring.

## 2 SEXTUPOLE EFFECTS

The most common magnet non-linearity encountered in small rings arises from high-field sextupoles introduced for chromaticity control. The SNS ring contains twenty chromatic sextupoles, placed in the arcs in high  $\beta$  and dispersion areas [4]. Their non-linear effect has been quantified and found small. Sextupole-like contributions also come from the leading-order fringe-field effect of the thirty-two arc dipoles. These sextupole effects, also small, can easily be corrected by the eight dedicated sextupole correctors.

## 3 OCTUPOLE-LIKE EFFECTS

The “kinematic non-linearity” refers to high-order terms in the expansion of the classical relativistic Hamiltonian

which contain only the transverse momenta,  $p_x$  and  $p_y$ . This non-linearity is negligible in high-energy colliders (*e.g.* RHIC, LHC), where  $p_{x,y} \ll p_z$ ; but in the SNS it is not so small [5]. By keeping all the kinematic terms in the expansion of the Hamiltonian, we obtain a general expression for the first-order tune-shift they induce:

$$\delta\nu_{x,y} = \frac{1}{2\pi} \sum_{k=2}^{\infty} \frac{(2k-3)!!}{2^k(2k)!!} \times \sum_{\lambda=0}^k \lambda \binom{2\lambda}{\lambda} \binom{k}{\lambda} \binom{2(k-\lambda)}{k-\lambda} J_{x,y}^{\lambda-1} J_{y,x}^{k-\lambda} G_{x,y} \quad (1)$$

where  $G_{x,y} = \oint_{\text{ring}} \gamma_{x,y}^{\lambda} \gamma_{y,x}^{k-\lambda} ds$  depends on the usual Twiss gamma functions. The first, usually dominant, term in the series gives an octupole-like tune-shift, *i.e.* linear in the actions. For the SNS ring, where the emittance is large and the gamma functions in the straight sections exceed unity, the kinematic terms give a small tune-shift of about  $10^{-4}$  at  $480\pi \text{ mm} \cdot \text{mr}$ , a value confirmed by both the analytical expression (1) and numerical simulations [3].

The relative impact of a longitudinal fringe field on a particle's transverse momentum is proportional to the ratio of transverse emittance to magnetic length [6]. Hence, the effect of quadrupole fringe-fields is usually small in low-emittance, low aspect-ratio machines (*e.g.* RHIC, LHC) but is very important for high-emittance, high aspect-ratio machines such as the SNS. For a quadrupole one can evaluate the fringe-field contribution in the limit of zero fringe length. The corresponding Hamiltonian for a single fringe (to leading order) is [7, 8]

$$H_f = \frac{\pm Q}{12B\rho(1+\frac{\delta p}{p})} (y^3 p_y - x^3 p_x + 3x^2 y p_y - 3y^2 x p_x), \quad (2)$$

where  $Q_i$  is the quad strength, and the + and – signs are used at, respectively, the entrance and exit of the magnet. It follows, as Lee-Whiting showed many years ago [9], that a quadrupole fringe-field induces an octupole-like transverse kick. Using MARYLIE [10], one can build quadrupole maps that include fringe fields based on either (2) or an exact representation [11]. We created tune footprints by applying Laskar's frequency analysis [12] to 1200 turns of MARYLIE tracking data. Particles were launched in different directions out to  $1000\pi \text{ mm} \cdot \text{mr}$ , and the only non-linearities included were those caused by thick elements and magnet fringe fields. Figure 1 shows that quadrupole fringe fields have an important impact on the dynamics of the SNS ring, giving tune spreads of about (0.04,0.03) at

\* Work supported by the U. S. Department of Energy

<sup>†</sup> papap@bnl.gov

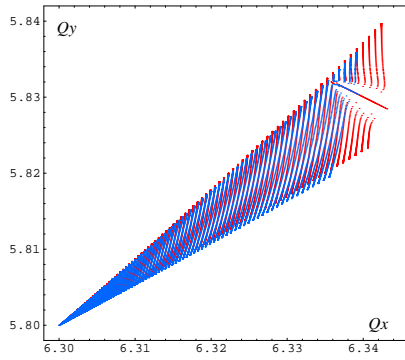


Figure 1: Tune footprints of the SNS ring, based on realistic (blue) and hard-edge (red) quadrupole fringe fields.

$1000\pi \text{ mm} \cdot \text{mr}$ , roughly one-third the space-charge tune spread [5]. In addition, Fig. 1 shows that the hard-edge model slightly overestimates the fringe-field effect and therefore represents a conservative estimate.

In our case the tune spread can be accurately represented by the results of first-order perturbation theory [7, 8]:

$$\begin{pmatrix} \delta\nu_x \\ \delta\nu_y \end{pmatrix} = \begin{pmatrix} a_{hh} & a_{hv} \\ a_{hv} & a_{vv} \end{pmatrix} \begin{pmatrix} 2J_x \\ 2J_y \end{pmatrix}, \quad (3)$$

where the normalized anharmonicities are given by

$$\begin{aligned} a_{hh} &= \frac{-1}{16\pi B\rho} \sum_i \pm Q_i \beta_{xi} \alpha_{xi}, \\ a_{hv} &= \frac{1}{16\pi B\rho} \sum_i \pm Q_i (\beta_{xi} \alpha_{yi} - \beta_{yi} \alpha_{xi}), \\ a_{vv} &= \frac{1}{16\pi B\rho} \sum_i \pm Q_i \beta_{yi} \alpha_{yi}. \end{aligned} \quad (4)$$

Here the index  $i$  runs over the entrances and exits of all quadrupoles in the ring, and the  $+$  and  $-$  signs are as in (2). Note that the entrance and exit fringe fields do *not* cancel one another: even if the  $\beta$  functions are equal at the entrance and exit, the  $\alpha$  functions usually change sign, leading to an additive effect. For the SNS lattice we find  $(a_{hh}, a_{hv}, a_{vv}) \approx (49, 22, 42) \text{ m}^{-1}$ , and these values closely match (apart from the obvious resonance) the results shown in Fig. 1.

## 4 OCTUPOLE CORRECTION

Octupole magnets can modify the tune-spread caused by quadrupole fringe-fields, kinematic non-linearity, chromatic sextupoles, and other octupole-like effects. If octupoles are placed in non-dispersive areas, the anharmonicities (4) become

$$\begin{aligned} A_{hh} &= a_{hh} + \frac{3}{16\pi B\rho} \sum_j O_j \beta_{xj}^2, \\ A_{hv} &= a_{hv} - \frac{6}{16\pi B\rho} \sum_j O_j \beta_{xj} \beta_{yj}, \\ A_{vv} &= a_{vv} + \frac{3}{16\pi B\rho} \sum_j O_j \beta_{yj}^2. \end{aligned} \quad (5)$$

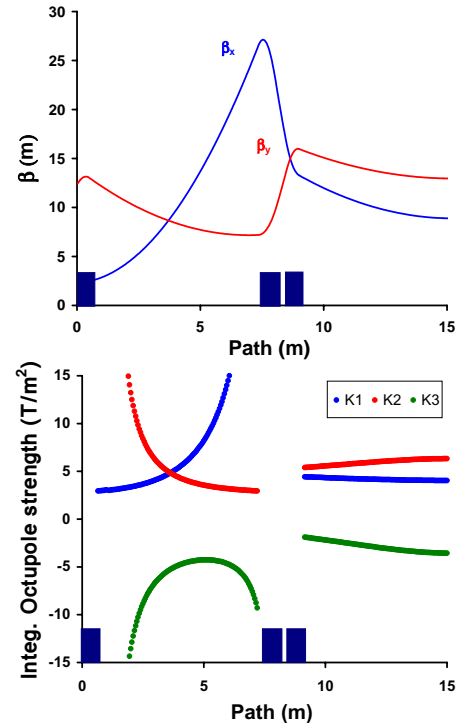


Figure 2: Top: the  $\beta$  functions in the first half of the SNS straight section. Bottom: integrated strengths of three families of octupoles versus location of the third family.

Here  $O_j$  denotes integrated octupole strength, and the index  $j$  runs over all octupoles in the ring. Complete cancellation of the tune-spread requires three families of octupoles to drive the anharmonicities (5) to zero. In some cases, when one anharmonicity is much smaller than the others, two families of octupoles can reduce the tune-spread. This is not the case for the SNS ring, where a third family must be added to the two already present.

The octupole strengths required to drive the anharmonicities (5) to zero depend on the octupole locations. Figure 2 shows the integrated strengths of the octupole correctors versus the position of the third family in one of the SNS ring straight sections. The first two families, at the ends of each arc, are located where  $\beta_x$  and  $\beta_y$  take extremal values. Then the optimal position for the third corrector is where the  $\beta$  functions are roughly equal, *i.e.* either in the middle of the straight section or just after the doublet.

## 5 DODECAPOLE ERRORS

In a magnet with normal quadrupole symmetry the first allowed multipole error is the normal dodecapole,  $b_6$ . In the absence of pole-tip shaping, this error can be exceedingly large: for the SNS 21 cm quadrupole (see Fig. 3), an OPERA-3d [13] simulation (with un-shaped ends) gives a dodecapole component of about 120 (in units of  $10^{-4}$ , normalized with respect to the main, quadrupole, component).

Because the dodecapole error is quite localized, its effect can be computed using a thin-element approximation. Applying first-order perturbation theory, one finds the tune-

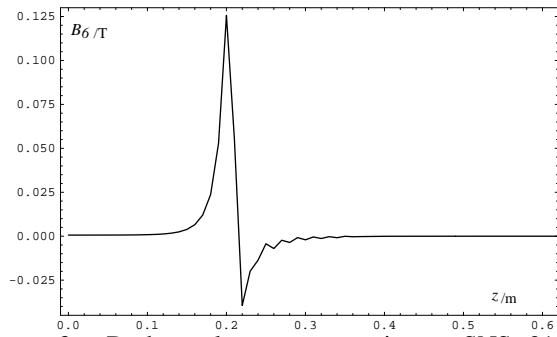


Figure 3: Dodecapole component in an SNS 21 cm quadrupole with un-shaped ends. The reference radius is 10 cm, and the origin,  $z = 0$ , is at the magnet's center.

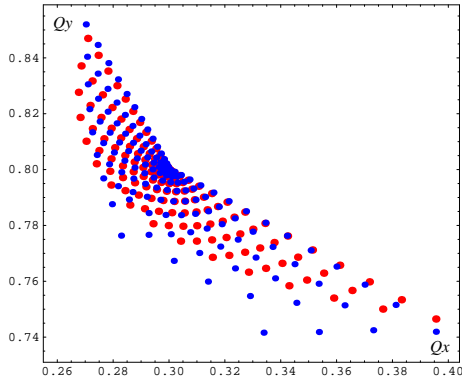


Figure 4: Tune footprints of the SNS ring with a dodecapole error in the quadrupoles of  $b_6 = 60$  units; results are from tracking data (blue) or the analytic result (6) (red).

spread induced by dodecapole errors is given by

$$\begin{pmatrix} \delta\nu_x \\ \delta\nu_y \end{pmatrix} = \sum_i \frac{b_{6i} Q_i}{8\pi B\rho} \mathcal{D}_i \begin{pmatrix} J_x^2 \\ J_x J_y \\ J_y^2 \end{pmatrix}, \quad (6a)$$

where  $\mathcal{D}_i$  denotes the  $3 \times 2$  matrix

$$\begin{pmatrix} \beta_{xi}^3 & -6\beta_{xi}^2\beta_{yi} & 3\beta_{xi}\beta_{yi}^2 \\ -3\beta_{xi}^2\beta_{yi} & 6\beta_{xi}\beta_{yi}^2 & -\beta_{yi}^3 \end{pmatrix}. \quad (6b)$$

Here the index  $i$  runs over all dodecapole kicks in the ring, *i.e.* over the entrances and exits of all quadrupoles. Note that this effect depends linearly on the error strength, but quadratically on the amplitude. In Fig. 4 a comparison of this analytic result with MARYLIE tracking data<sup>1</sup> shows a striking agreement. Figure 4 also shows that the very large uncorrected dodecapole error gives a tune-spread (at  $1000\pi \text{ mm} \cdot \text{mr}$ ) roughly twice that caused by the quadrupole fringe fields.

By shaping the ends of the quadrupoles, one can reduce the  $b_6$  error to 1 unit or less [14]. Such shaping reduces the peak and the trough seen in Fig. 3, and makes those two areas roughly cancel one another. This constitutes *local* compensation. One might also correct the  $b_6$  error by adding a small negative dodecapole component through the body of the magnet. In Fig. 5 we compare the tune-spreads

<sup>1</sup>The dodecapole kicks were generated by a MARYLIE user routine.

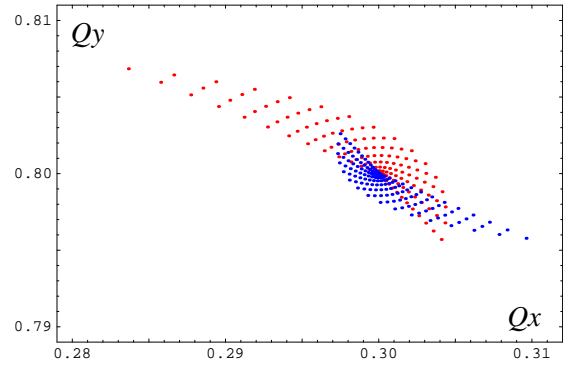


Figure 5: Comparison of tune-shift plots using body (red) and local (blue) compensation of the dodecapole component in the SNS ring quadrupoles.

(6) after local and body compensation. In this example, the compensation works well in both cases, with local compensation being slightly better. But, in fact, it is essential to use local compensation: because the tune-spreads (6) depend cubically on the  $\beta$  functions, the results of body compensation will be very sensitive to the ring optics.

## REFERENCES

- [1] J. Wei et al., A FODO/Doublet Lattice for the SNS Accumulator Ring, these Proceedings.
- [2] J. Wei et al., Phys. Rev. ST Accel. Beams (accepted).
- [3] A. Fedotov et al., Effect of non-linearities on beam dynamics in the SNS accumulator ring, these Proceedings.
- [4] N. Tsoupas et al., Chromatic correction and optical compensation in the SNS accumulator ring using sextupoles, these Proceedings.
- [5] A. Fedotov et al., Halo and space-charge issues in the SNS accumulator ring, these Proceedings.
- [6] J. Wei et al., Scaling law for the impact of magnet fringe field, these Proceedings.
- [7] E. Forest, J. Milutinovic, Nucl.Inst. and Meth. A269, 474, 1988.
- [8] E. Forest, *Beam Dynamics - A new attitude and framework*, Harwood Acad. Pub., Amsterdam, 1998.
- [9] G.E. Lee-Whiting, Nucl.Inst. and Meth. 103, 117, 1972.
- [10] A.J. Dragt, et al., *MARYLIE 3.0 User's Manual*, University of Maryland, Physics Department Report, 1999.
- [11] M. Venturini, A. Dragt, Nucl.Inst. and Meth. A427, 387, 1999.
- [12] J. Laskar, Physica D 67, 257 (1993); J. Laskar and D. Robin, Part. Acc. 54, 183 (1996).
- [13] Vector Fields, Ltd, Oxford England.
- [14] K.G. Steffen, *High Energy Beam Optics*, Interscience, New York, 1965.